Precambrian Research 244 (2014) 23–32

Contents lists available at ScienceDirect

Precambrian Research

journal homepage: www.elsevier.com/locate/precamres

On the low-inclination bias of the Precambrian geomagnetic field

Toni Veikkolainen [a,*], David A.D. Evans [b], Kimmo Korhonen [c], Lauri J. Pesonen [a]

[a] Division of Geophysics and Astronomy, Department of Physics, University of Helsinki, FI-00014 Helsinki, Finland
[b] Department of Geology and Geophysics, Yale University, New Haven, CT 06511, USA
[c] Geological Survey of Finland, FI-02151 Espoo, Finland

ARTICLE INFO

Article history:
Received 20 February 2013
Received in revised form 2 September 2013
Accepted 3 September 2013
Available online 12 September 2013

Keywords:
Geocentric Axial Dipole
Non-dipole
Quadrupole
Octupole
Zonal
Inclination

ABSTRACT

A long tradition has emerged in applying the inclination frequency analysis to estimate the functionality of the Geocentric Axial Dipole (GAD) hypothesis in paleomagnetism. In the present study, the theory has been tested to the database with 3246 records of the Precambrian geomagnetic field. To find the best-fitting inclination distribution, different combinations of geocentric axial dipolar (GAD), quadrupolar (G2) and octupolar (G3) spherical harmonics have been analyzed. The influence of various factors on the inclination distribution has been studied, including the geologic age, rock type, magnetic polarity, quality of data and their spatiotemporal distribution. By two-dimensional chi-square analysis on crystalline rocks only, which avoid problems associated with remanence shallowing among sedimentary rocks, the most plausible estimates for the zonal non-dipolar contributions of the field have been determined as 2% for G2 and 5% for G3, values much lower than in previous estimates using the same method. However, the inherent non-uniqueness of the inclination frequency analysis and the uneven spatiotemporal sampling of the field around the globe during the Precambrian necessitate other independent methods of testing the GAD hypothesis.

1. Introduction

The introduction of the GAD hypothesis has been mainstream in paleomagnetism since its very beginning. Its validity in various geological timescales has been tested e.g. using sedimentary paleoclimatic indicators of latitude (Evans, 2006), virtual axial dipole moment (Donadini et al., 2007), scatter of virtual geomagnetic poles (VGPs) as a function of paleolatitude (Biggin et al., 2008; Smirnov et al., 2011) or reversal asymmetries (Nevanlinna and Pesonen, 1983). One of the most commonly employed tests is the global inclination frequency analysis (e.g. Evans, 1976), which is based on the fact that the average geomagnetic field can be described as a combination of zonal harmonic terms and each set of them generates a distinct inclination frequency distribution, where the absolute value of inclination ($|I|$) is shown as a function of its proportion. This method is advantageous since it uses a simple measurable property (inclination) of the geomagnetic field and can be extended to the Precambrian eon. To create a discrete distribution of $|I|$, the real or synthetic dataset must be classified into intervals. The choice is arbitrary, but 10-degree intervals have been generally used (e.g. Kent and Smethurst, 1998). Distributions for pure axial dipole (g_1^0), quadrupole dipole (g_2^0) and octupole (g_3^0) are based on Eq. (1) and shown in Fig. 1. In the equation, P_n stands for the Legendre polynomial of the n:th spherical harmonic degree and θ for paleocolatitude of the sampling site (Merrill et al., 1998).

$$\tan I = \frac{P_n(1+n)}{\partial P_n/\partial\theta} \quad (1)$$

In this analysis, the sign of inclination is not taken into account, since the sign of paleolatitudes (90°-θ) cannot be properly determined for Precambrian data due to insufficient knowledge of continental or cratonic motions. Theoretical curves of $|I|$ have a peak at mid- to high inclinations ($60^\circ \le |I| \le 70^\circ$) because the field equations for g_1^0, g_2^0 and g_3^0 are nonlinear, as are the areas between various latitude circles. For example, in the case of a pure GAD field, if a statistically significant amount of inclination data have been gathered from random locations, ca. 8.8% of those should fall into the interval $0^\circ \le |I| < 10^\circ$, but only 5.7% into the interval $80^\circ \le |I| \le 90^\circ$. A more detailed view of the geomagnetic field requires that superpositions, i.e. combinations of axial dipolar, quadrupolar and octupolar fields of different strengths, are considered. Distributions caused by higher multipoles, such as g_4^0, however, cannot be applied to studies of the Precambrian in a meaningful way, as the spatiotemporal limitations of the data available do not allow a detailed spherical harmonic analysis to be done.

The effect of a small quadrupole on the inclination frequency distribution is considered minor (Fig. 2). However, the contribution of g_2^0 to the inclination observed at a given paleolatitude is

* Corresponding author. Tel.: +358 40 7645113.
E-mail address: toni.veikkolainen@helsinki.fi (T. Veikkolainen).

0301-9268/$ – see front matter © 2013 Elsevier B.V. All rights reserved.
http://dx.doi.org/10.1016/j.precamres.2013.09.004

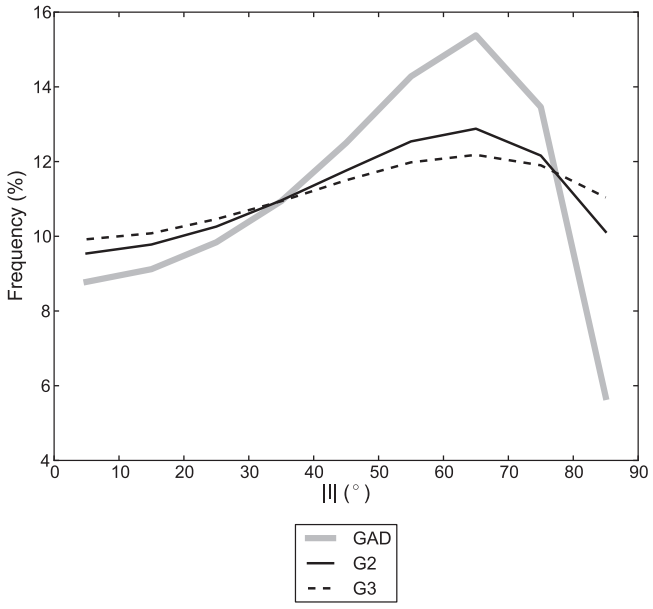

Fig. 1. Inclination distributions for pure dipolar, quadrupolar and octupolar fields. Frequencies within the 10-degree bins according to Evans (1976).

much more significant and similar on both hemispheres due to the symmetry of g_2^0 about the equator, leading to negative inclination anomalies if g_1^0 and g_2^0 are parallel, or to positive anomalies if they are antiparallel. Small octupolar fields, on the other hand, do not strongly alter local paleolatitudes, but do have a noticeable effect on the inclination frequency distribution. Practically the presence of a slight axial geocentric octupole of the same sign as the dipole (and presumed to reverse polarity coincident with the dipole) means that inclinations obtained from mid-latitude observations are systematically too shallow. On the contrary, the presence of a small octupole with a sign opposite to that of GAD (reversing along with the dipole always to maintain its opposite sign) steepens

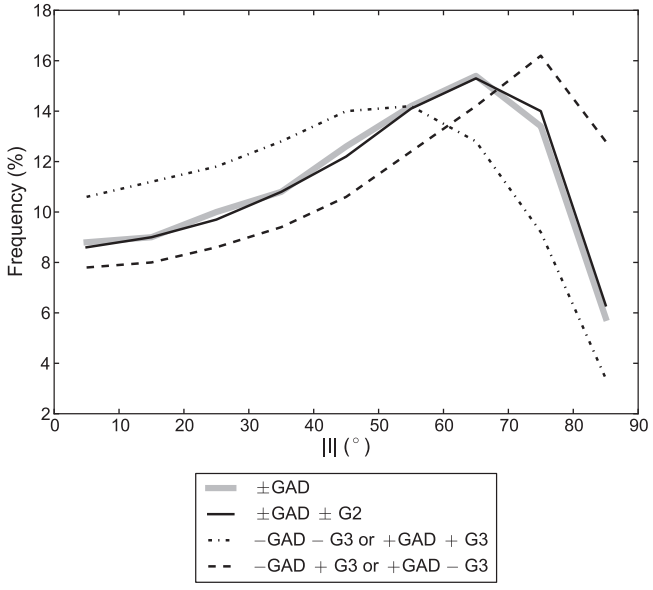

Fig. 2. Inclination distributions for pure GAD (±30,000 nT), and multipole models, where G2 and |G3 are 10% of the strength of GAD. Solid black line: negative or positive GAD with a negative or positive quadrupole. Dot-dashed black line: negative GAD with a negative octupole, or positive GAD with a positive octupole (g_3^0 parallel with g_1^0). Dashed black line: Negative GAD with a positive octupole, or positive GAD with a negative octupole (g_3^0 antiparallel with g_1^0).

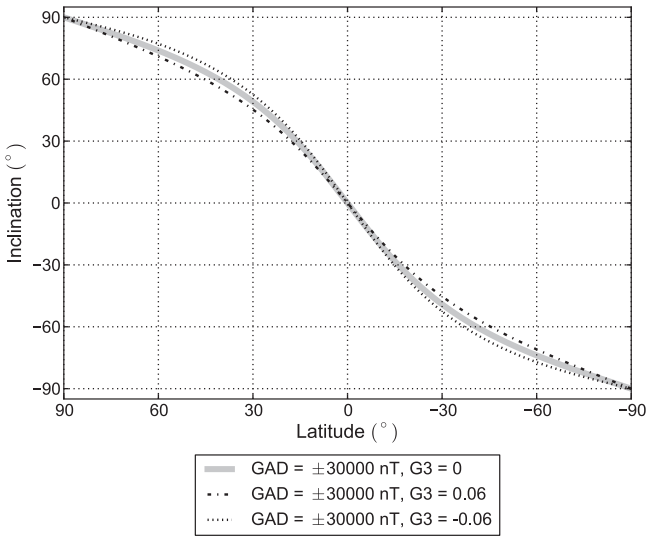

Fig. 3. Inclination vs paleolatitude for a permanent 6% octupole field model. Dot-dashed line describes the situation where g_1^0 and g_3^0 are of the same sign and dotted line describes the situation where they are of the opposite sign.

inclinations from those resulting from pure GAD, as demonstrated by Fig. 3. A combination of permanent (standing) quadrupolar and octupolar components (or alternatively modelled as an axial, eccentric, non-reversing subsidiary dipole) was used by Nevanlinna and Pesonen (1983) to explain the steepened R and shallowed N directions observed in the Late Mesoproterozoic Keweenawan rocks. The present study, however, follows earlier database-wide inclination frequency analyses in considering only axial and geocentric field harmonics, with "odd" terms such as the octupole reversing so as to maintain a consistent polarity relationship to the dominant dipole component.

In the inclination frequency method, geomagnetic declinations are neglected, since by definition, the model uses zonal harmonics only, and these are not influenced by the geographic longitude. Even if there were non-zonal harmonics too, declination is very poorly constrained in the vicinity of geomagnetic poles and values of D from different paleolatitudes should first be reduced to a single latitude to be useful in statistical calculations. The rejection of declination means that the method cannot distinguish between different types of dipolar fields. For example, inclination distributions resulting from a GAD field and a tilted, or equatorial geocentric dipole field are equal. This demonstrates the fact that as long as the field is sampled spatiotemporally adequately enough, the inclination distribution remains unchanged even if the field is being rotated. Therefore other methods, such as paleosecular variation studies (Tauxe and Kodama, 2009; Smirnov et al., 2011) and asymmetries in dual-polarity paleomagnetic results (Khramov and Iosifidi, 2012; Veikkolainen et al., 2013a) must be used to determine possible equatorial dipoles and other non-zonal features of the field.

For most purposes, it is useful not to express the absolute strengths of spherical harmonic terms, but to normalize them with the GAD component (g_1^0). In the case of zonal fields only, these are denoted using capital letters and numbers, such as G2 for g_2^0/g_1^0 and G3 for g_3^0/g_1^0. For example, Kent and Smethurst (1998) modelled the mean geomagnetic field of Paleozoic (250–542 Ma) and Precambrian (>542 Ma) together using terms G2 = 0.10 and G3 = 0.25. This cannot be considered to be just a minor adjustment to the GAD hypothesis. It would require a significant change in the magnetohydrodynamic conditions to have taken place, since an analysis of rocks from the past 210 Ma suggests G3 to be not more than 3 ± 8% (Courtillot and Besse, 2004). A study on the

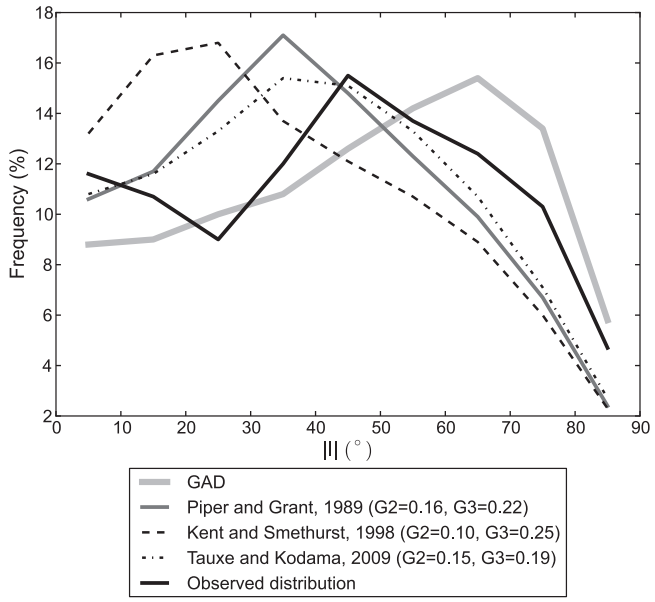

Fig. 4. Inclination frequency distributions from previous studies on the Precambrian geomagnetic field, compared with the observed distribution resulting from our data.

Permian and Triassic paleomagnetic data also shows a fairly small deviation from the GAD model, with an axial octupole G3 = 0.10, though this conclusion is based on European and Siberian data only (Veselovskiy and Pavlov, 2006). However, analyses of the time-averaged field of 0. . .5 Ma have persistently revealed a standing, positive value of G2 (Carlut and Courtillot, 1998; Hatakeyama and Kono, 2002; McElhinny, 2004), typically ranging from 0.04 to 0.08. In the least squares analysis based on inclination values from continental igneous rocks and ocean cores, McElhinny (2004) determined the temporal mean of G3 for the past 5 Ma to be just 0.011 ± 0.012, thus questioning the statistical significance of the axial octupolar term in the time-averaged field.

For the Cenozoic (0–65 Ma) data, Kent and Smethurst (1998) fitted a zonal model statistically indistinguishable of GAD. The increasingly dipolar character of the field in the 250 Ma was explained by the growth of inner core, which stabilized the geodynamo and made the non-dipolar fields decline. The success of GAD in explaining the database-wide inclination frequencies must also be partly due to a surprisingly even distribution of continental area as a function of paleolatitude in these relatively short geologic timescales. As the axial quadrupole is a symmetric term, superpositions with GAD + G2 and GAD-G2 are equal, irrespective of the sign of G2. Actually it has been estimated that the magnitude of G2 has, in the past 200 Ma, varied between the values −0.14 and 0.10, depending on the model (Livermore et al., 1984). Conversely, the axial octupolar term is antisymmetric about equator, and hence the inclination distribution of GAD and an axial octupole is dependent on the signs of g_1^0 and g_1^0 (Fig. 2).

As seen in Figs. 2 and 3, even a small axial octupolar term, if axial and consistently of the same sign with g_1^0, clearly shifts the inclination data towards lower values. This phenomenon, referred to as low-inclination bias, has been problematic already after the publication of first inclination frequency analyses of GAD. Previous database-wide inclination studies (Piper and Grant, 1989; Kent and Smethurst, 1998; Tauxe and Kodama, 2009) optimized values of G2 and G3 to fit the Precambrian distributions, obtaining values between 10% and 25% for both parameters (Fig. 4). Alternatively, low inclinations may be caused by the anisotropy in sampled rocks (Cogné et al., 1999), or sedimentary inclination flattening (Kodama, 2012). Uneven spatial distributions of preserved rocks may also explain the low-inclination bias: Kent and Smethurst (1998), for example, suggested that another possible explanation was the preferential location of continents at low latitudes through the supercontinent cycle, via the process of true polar wander (see also Evans, 1998, 2003). Because true polar wander induces relative sea-level shifts that are transgressive at low latitudes (Wegener, 1929, p.159–163), sedimentary basins may also be preferentially located near the equator. It has also been suggested that the continental drift has not occurred for such a long time that a position of a single continent can be considered random in the long run (Meert et al., 2003; McFadden, 2004). Whenever chi-square statistics are applied for analyzing the validity of the GAD hypothesis, a warning must be given since the testing method is inherently very sensitive to the sample size. Since large datasets very regularly cause the critical value of the test statistic χ^2 to be exceeded, even in cases where the observed and theoretical distributions are nearly equal in appearance, various additional methods have been suggested, including the Hoelter index as applied by Meert et al. (2003).

2. Data and modelling

This study uses paleomagnetic data from the novel Precambrian database collected by University of Helsinki and Yale University (Pesonen et al., 2012a; Veikkolainen et al., 2013b), with 3246 observations from different continents, continental fragments and cratons globally. By comparison, earlier studies using this method analyzed the following number of Precambrian data: 1277 (Kent and Smethurst, 1998; using the Global Paleomagnetic Database (GPMDB) of McElhinny and Lock, 1996) and 1362 (Grower, 2005; using the updated version of GPMDB (Pisarevsky, 2005). Our (dataset is substantially larger, because we have incorporated results from ten years beyond earlier compilations (2003–2013), and we have also integrated some archival pre-2003 data that were omitted from GPMDB.

The selection of paleomagnetic data for statistical purposes needs to be done carefully, since one must not treat all observations in an equal manner. Hence the first step in our prefiltering was to remove subentries of so-called combined results, which are very frequent especially in Soviet paleomagnetic catalogue data. For example, the entry of Utchur River sediments (result 5662 in GPMDB) has three subentries: 5659, 5660 and 5661. Another thing to take into account was the fact that our database had several combinations of normal- and reversed-polarity data in cases with obvious or suspected magnetic field reversals. In these situations the combined entry generally superseded the individual N and R subentries, although a few exceptions remained. These include e.g. Jänisjärvi impactites, which have a normal-polarity direction with $D = 59.4^\circ$, $I = 69.6^\circ$, and a reversed-polarity direction with $D = 222.1^\circ$, $I = -38.7^\circ$. Since the resulting angle between N and R directions is 148° rather than 180° predicted by GAD, and ages of N and R units are not precisely known, it remains suspicious whether these observations represent an actual polarity change of the field, or whether they represent distinctly different moments of geologic time. The substantial role of prefiltering in removing obvious duplicates is well demonstrated by the fact that the original set of 3246 records was reduced to 2596.

Before the analysis, all entries were ranked according to their reliability in the MV ("Modified Van der Voo") grading: among seven quality factors described by Van der Voo (1990), the seventh, that is, lack of similarity to younger poles, is not considered here. This is due to the fact that Precambrian paleomagnetic poles of clearly different ages may commonly match each other very closely on the globe, as demonstrated for example by results from the Lake Superior region (Ernst and Buchan, 1993) and southern Scandinavia (Pisarevsky and Bylund, 2006). In addition, for longer

Table 1
Comparison of inclination distributions for (a) igneous (i), sedimentary (s) and metamorphic (m) rocks, (b) igneous rocks with positive (+) and negative (−) inclinations. In (b) cases, N and R have been regarded as separate entries, when polarity pairs are concerned. Results with MV ≥ 3 included, no poorer-quality data. The values of the test statistic X^2 calculated using a GAD as a null hypothesis. See also Figs. 5 and 6.

Interval	i	s	m	i (+)	i (−)
$0 \le \lvert I \rvert < 10^\circ$	101 (11.2%)	80 (19.3%)	13 (15.5%)	49 (9.0%)	52 (14.5%)
$10 \le \lvert I \rvert < 20^\circ$	101 (11.2%)	59 (14.2%)	8 (9.5%)	46 (8.4%)	55 (15.4%)
$20 \le \lvert I \rvert < 30^\circ$	94 (10.4%)	60 (14.4%)	6 (7.1%)	54 (9.9%)	40 (11.2%)
$30 \le \lvert I \rvert < 40^\circ$	110 (12.2%)	72 (17.3%)	5 (6.0%)	74 (13.6%)	36 (10.1%)
$40 \le \lvert I \rvert < 50^\circ$	140 (15.5%)	54 (12.9%)	7 (8.3%)	90 (16.5%)	50 (14.0%)
$50 \le \lvert I \rvert < 60^\circ$	102 (11.3%)	53 (12.7%)	14 (16.7%)	70 (12.8%)	32 (8.9%)
$60 \le \lvert I \rvert < 70^\circ$	112 (12.4%)	19 (4.6%)	20 (23.8%)	78 (14.3%)	34 (9.5%)
$70 \le \lvert I \rvert < 80^\circ$	97 (10.7%)	19 (4.6%)	8 (9.5%)	50 (9.2%)	47 (13.1%)
$80 \le \lvert I \rvert < 90^\circ$	46 (5.1%)	1 (0.0%)	3 (3.6%)	34 (6.2%)	12 (3.3%)
Combined	903 (100%)	417 (100%)	84 (100%)	545 (100%)	358 (100%)
X^2	35.921	165.296	12.221	19.714	50.065
p-Value	<0.0001	<0.0001	0.1416	0.0115	<0.0001

time intervals such as Precambrian, decision on whether a "younger pole" is in itself reliable, can be highly subjective. Quality filtering of the database represents a trade-off between the reliability of results versus the limited number of entries in a highly selective subset: if filtering is too severe, then analysis suffers from the statistics of small data, contradicting even the premise of the test (i.e. adequate random sampling by continents across the surface of the Earth). A more detailed discussion of the effects of quality filtering will follow, but as an initial compromise, we focused our analyses on a subset of MV ≥ 3 (out of a six-point total). We find that altogether just over 1400 observations from igneous, sedimentary and metamorphic rocks pass such quality criteria (Table 1).

Several factors hamper statistical analyses of paleomagnetic inclination data. First, the observations are distributed both spatially and temporally very unevenly, especially when considering the long timespan of the Precambrian. Second, many directional studies have been performed multiply on the same rocks; the Keweenawan succession in North America is one of the numerous examples. To overcome this, both Kent and Smethurst (1998) and Grower (2005) applied spatiotemporal binning to the most recent versions of the GPMDB. Kent and Smethurst (1998) divided the globe into sections with 10-degree latitudinal and longitudinal dimensions, and split the Precambrian into 50 Ma time windows. Within each bin, absolute values of inclinations were averaged. As a result, their original Precambrian dataset of 1277 observations was reduced to 531 even though individual entries were not filtered using any reliability scale. This purely mathematical procedure, incorrectly based on present-day geography, not only fails to recognize the cratonic boundaries within a single continent, but it also causes high-quality results to be mixed with highly suspicious observations.

Table 2
Inclination distributions for rocks from different geological eras (Archean, Paleoproterozoic, Mesoproterozoic and Neoproterozoic). Only i + m, MV ≥ 3. The values of the test statistic X^2 calculated with GAD as a null hypothesis. See also Fig. 7.

Interval	Archean	Paleoprot.	Mesoprot.	Neoprot.
$0 \le \lvert I \rvert < 10^\circ$	6 (9.4%)	48 (12.5%)	38 (11.6%)	22 (10.5%)
$10 \le \lvert I \rvert < 20^\circ$	5 (7.8%)	43 (11.2%)	41 (12.5%)	20 (9.5%)
$20 \le \lvert I \rvert < 30^\circ$	4 (6.3%)	36 (9.4%)	39 (11.9%)	21 (10.0%)
$30 \le \lvert I \rvert < 40^\circ$	5 (7.8%)	41 (10.7%)	43 (13.1%)	26 (12.4%)
$40 \le \lvert I \rvert < 50^\circ$	8 (12.5%)	50 (13.0%)	61 (18.5%)	28 (13.3%)
$50 \le \lvert I \rvert < 60^\circ$	9 (14.1%)	60 (15.6%)	24 (7.3%)	23 (11.0%)
$60 \le \lvert I \rvert < 70^\circ$	13 (20.3%)	54 (14.1%)	37 (11.2%)	28 (13.3%)
$70 \le \lvert I \rvert < 80^\circ$	11 (17.2%)	27 (7.0%)	36 (10.9%)	31 (14.8%)
$80 \le \lvert I \rvert < 90^\circ$	3 (4.7%)	25 (6.5%)	10 (3.0%)	11 (5.2%)
Combined	64 (100%)	384 (100%)	329 (100%)	210 (100%)
X^2	4.575	22.054	42.578	4.070
p-Value	0.802	0.005	<0.0001	0.851

The major shortcoming of spatial binning by present site latitude and longitude is the fact that it can mingle results from originally far-separated cratons. As an example, in the Slave craton, the Caribou lake gabbro (Irving et al., 1984) has the U–Pb age of 2186 ± 10 Ma; while in the Superior craton, the Biscotasing West dykes (Halls and Davis, 2004) are 2167.8 ± 2.2 Ma. The current sampling sites of these similarly aged rocks are less than 500 km apart, but the respective paleomagnetic poles differ by 7600 km (68°) on the globe. In other words, paleomagnetic data are strongly in favour of the independent drift of Slave and Superior cratons at ca. 2.17 Ga, before the unification of Laurentia (Buchan et al., 2009). In carrying out spatiotemporal binnings, these results, must not be combined. The binning must be done on the basis of all cratons separately, unless they can be validated to have been parts of a common tectonic plate. The key requirement of the binning is the sufficient knowledge of the geologic unit of each entry, and we have paid particular attention to this property when constructing our database. In terms of geologic time, the binning should be ideally used for data which has already been quality filtered, since most paleomagnetic data, especially those of poor quality, have vague age constraints and therefore using e.g. a 50 Ma bin as suggested by Kent and Smethurst (1998) would not make sense. Hence we have applied the binning procedure only for data with MV ≥ 4, since the ages of moderate- and high-quality entries are in most cases more precisely known, and even in cases where no isotopic age is available, the age can be estimated using the APWP of the respective craton.

Another problem arises when data from both polarities should be included and they show an asymmetry, either in inclination, in declination or in both. This may arise from several reasons (see discussion by Veikkolainen et al., 2013a) but here we are concerned with the effect of age difference between "locking-in" of N and R polarity magnetizations. The age difference, if substantial, can produce remanence vectors with considerable differences from a purely antipodal case. Rapidly deposited lavas or sediments most likely do not reveal considerable departures from antipodality, but have their magnetization directions or poles within conventional secular variation scatter. However, if there are hiatuses, and thus considerable age differences in the lock-in times of magnetization between N and R units, allowing APWP to take place, the asymmetries between N and R units can be due to APW (continental drift) rather than any aspects of the geomagnetic field, such as non-dipole field. This problem is envisaged at least at the Mamainse Point volcanic section in the Keweenawan succession (Swanson-Hysell et al., 2009). In the North Shore lavas, overprinting by hematite is only visible in N magnetizations, thus supporting the theory of different ages of N and R directions (Tauxe and Kodama, 2009).

For the inclination analysis used in this paper, normal and reversed directions within a same rock unit have been combined to a mean direction if they differ less than 30 degrees on the surface of the Earth, and no evidence for their distinct acquisition ages have been obtained thus far. For example, using the combined entry for Mashonaland sills (Bates and Jones, 1996) can be justified. As a counterexample, the Central Arizona diabases (Donadini et al., 2011) have ages ranging from 1119 ± 10 (baddeleyite) to 1085 ± 5.2 Ma (zircon) (Donadini et al., 2012), and mean inclinations of 38.7° and −78.7° for two distinct polarities. These results, along with those of normal- and reversed-polarity Matachewan dykes (e.g. Halls and Palmer, 1990), have been used as separate entries in the analysis, since they clearly describe the geomagnetic field at different points of time. To study whether the sign of the inclination vector has an influence on the resulting distribution, we have also split the observations into distinct positive- and negative-inclination groups throughout the database. However, these cannot

be directly linked to N and R polarity groups, as absolute polarities are unknown for the Precambrian.

As the aim of the study was to find a best-fit model for the Precambrian geomagnetic field, Pearson's χ^2 (chi-square) testing turned out to be very useful. The data have been split into 10-degree intervals of inclination, as originally done by Evans (1976) and all subsequent studies of this kind, so there are 8 degrees of freedom. The test statistic X^2 is the sum of values calculated for each interval separately, as shown by Eq. (2):

$$X^2 = \sum_{i=1}^{n} \frac{(O_i - T_i)^2}{T_i} \quad (2)$$

Here n is the number of classes, O_i is the observed frequency and T_i is the theoretical frequency resulting from the GAD model. Absolute frequencies must be used instead of percentages, so O_i and T_i need to be of same size. With 95% confidence level, the critical value for X^2 is 15.507. This was used to estimate whether the null hypothesis (i.e. GAD is valid) should be accepted or rejected. The test statistic was not determined if the total number of observations in the dataset did not exceed 50, or alternatively, if there were less than five observations in at least three classes. For statistically significant datasets, X^2 was calculated using the observed distribution, and it was compared with that of a same-sized synthetic dataset, which was generated based on the GAD model (see tables). In each case, a two-variable analysis was made to find the Gauss coefficients (G2 and G3) that fit the observed distribution best. The method was based on calculating X^2 values for zonal fields with different strengths of G2 and G3, and the values, which most closely matched the observations, were selected to represent the geomagnetic field model. Most continents alone, especially the least observed ones (e.g. Rio de la Plata and South China), had highly variable datasets, which could not be modelled using any combinations of G2 and G3. This was mainly due to the limited spatiotemporal coverage of the data, a reason why the analysis must be applied to a global, not a regional database. In this paper, the cratonic binning method is introduced to ensure that the analysis is done in a paleogeographically correct way.

The main point in our binning was to calculate a Fisher mean from declination–inclination pairs within each time interval, and to use the resulting I as a binned value. Since inclination is a non-linear angular quantity, using simple arithmetic means of I would be incorrect and cause a severe low-inclination bias. Before calculating our binned dataset, we changed polarities of some entries in bins where antipodal or nearly antipodal directions have been present, meaning that the D value was turned by 180° and I value just changes its sign. This approach is justified in these geologically short timescales where the antipodality cannot be caused by the drift of the continent to the opposite side of the globe. We are aware that the continental drift, paleosecular variation and other factors may cause the directions to be more scattered in some time intervals than in others. Therefore depending on the amount of data, the reliability of age information, and the clustering of D and I values of nearly same-aged entries within a craton, we have applied a flexible temporal length for each bin, ranging from 0 to 25 Ma. For instance, we have calculated the binned I value of 40.8° for the predominantly normal-polarity Keweenawan data of 1100. . .1085 Ma, and binned I of 67.3° for the reversed-polarity Keweenawan entries ranging from 1110 to 1000 Ma, respectively. Since the N and R polarities form two distinct groups with clearly different $|I|$ values, it would be unwise to include them in same bin, even though their age range is not more than 25 Ma.

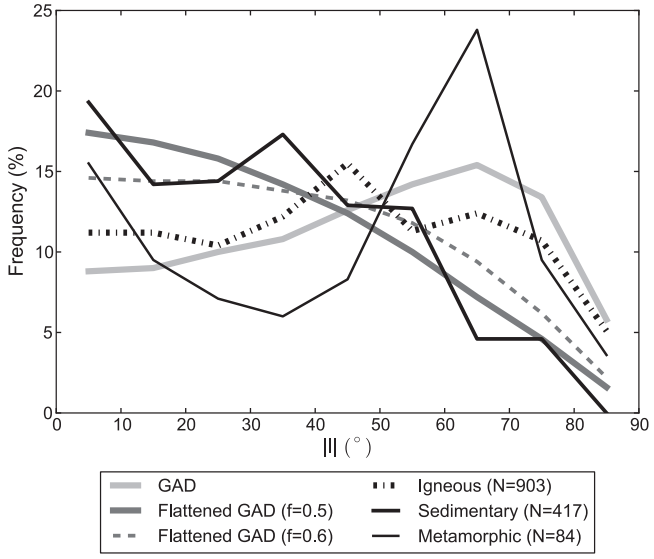

Fig. 5. Results from inclination analysis for igneous (i), sedimentary (s) and metamorphic (m) rocks from data of Table 1. MV ≥ 3 for all entries. The best statistical fit into igneous rock data is shown. In addition, King's law (King, 1955) has been applied to the GAD model to find the best fit to the observed sedimentary data. Curves with the flattening factor $f = 0.5$ (corresponding to the Precambrian) and $f = 0.6$ (corresponding to the Phanerozoic) are shown here.

3. Results

3.1. Rock type

To analyze how the chosen rock type affects the inclination distribution, all the data were divided into sedimentary (s), metamorphic (m) and igneous (i) rocks. Some continents, such as Baltica, India and Laurentia, are strongly dominated by igneous rocks, whereas Siberia, South China and Timan contain mainly sedimentary entries. As expected, the lowest bins of inclination were predominantly occupied by sedimentary data. Using King's law (King, 1955), the flattening factor f for sedimentary inclinations was calculated as:

$$\tan I_s = f \tan I \quad (3)$$

Here, the variable I is the original inclination, and I_s is the inclination affected by shallowing. For the Precambrian, the value of f that closely matches the observed sedimentary data (Table 1) was found to be 0.5 (Fig. 5) according to the chi-square analysis. This is comparable to the blanket factor of 0.6 applied to Phanerozoic sedimentary results by Torsvik et al. (2012), who chose that value to optimize the concordance of apparent polar wander paths derived from sedimentary versus crystalline rocks. The variability of the compaction rate of sediments may cause different-aged sediments to be subject to different degrees of inclination flattening, though the common lack of coeval igneous rocks in the same craton makes such comparisons difficult to assess in the Precambrian. Although not useful in inclination analysis, sedimentary strata can provide detailed time sequences of the reversals of the geomagnetic field (e.g. Bingham and Evans, 1976), and in fact, modelling Precambrian reversal data even provides a way to estimate the non-zonal geomagnetic at a given point of time (Komissarova et al., 1997).

In our data, sedimentary inclinations form distinct groups, e.g. the ca. 1.4 Ga Belt Supergroup in Wyoming (Elston et al., 2002) and formations, which are often temporally close to one another, e.g. Elatina, Nuccaleena, Brachina and Wonoka in late Neoproterozoic Australia (Schmidt et al., 1991; Schmidt and Williams, 2010). It has been observed that the spatial distribution of shallowed sedimentary inclinations is dissimilar to that resulting from a

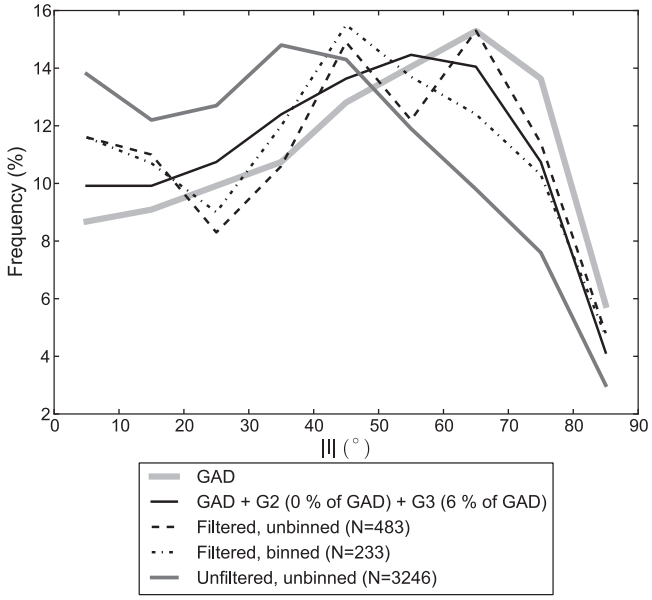

Fig. 6. Results from unbinned and binned observations of inclination for data from igneous (i) rocks, MV ≥ 4. In the best fit, the quadrupole (G2) is 0% and the octupole (G3) is 6% of GAD. The unbinned and unfiltered distribution with 3246 entries from all rock types is shown for comparison. When the quality filtering is done in a stricter way, the unbinned distributions are closer to GAD, as seen in Fig. 9.

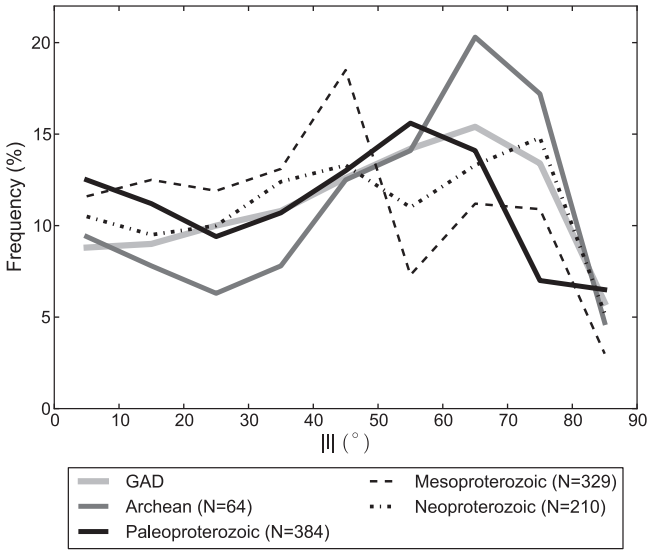

Fig. 7. Distributions of inclination for igneous rocks in four time windows: Archean (>2500 Ma), Paleoproterozoic (2500. . .1600 Ma), Mesoproterozoic (1600. . .1000 Ma) and Neoproterozoic (1000. . .542 Ma) from data seen in Table 2.

combination of GAD + G3, as evaluated from the elongation/inclination (*E*/*I*) theory (Tauxe and Kent, 2004). This method is based on the distinction of ellipticity in north-south direction, which is mainly caused by zonal multipoles, and the west-east elongation, which is more prominently a product of sedimentary inclination shallowing. In the vicinity of poles, the distributions of directions are circular. Schmidt et al. (2009) have shown that this theory can be effectively used for correcting flattened inclinations by comparing the observed values of inclination with the ellipticity that results from a geomagnetic model of the last 5 Ma, such as the predominantly dipolar TK03 model (Tauxe and Kent, 2004). In the inclination frequency analysis, however, inclinations altered by sedimentary shallowing are a source to a distribution with an equal appearance to that caused by a persistent non-dipolar field (e.g. Kent and Smethurst, 1998). Even in the case where sedimentary inclinations are excluded, the preference of very shallow inclinations $0° \leq |I| < 20°$ to moderately shallow ones $20° \leq |I| < 40°$ is clearly visible especially in the unbinned dataset (Fig. 6). Partly this is caused by the spatiotemporally insufficient sampling of Archean results, as seen in Fig. 7, but it also reflects the small number of individual observations in the lowest intervals of the distribution, and therefore a high sensitivity towards anomalous entries. This is strikingly different from the distribution of the unbinned and unfiltered dataset, which is very similar to that suggested by Kent and Smethurst (1998), and unlike all other ones in our study, based on raw data with no prefiltering. This casts more doubt on the Kent & Smethurst type binning.

3.2. Polarity

In the inclination frequency method, observations are generally handled regardless of the actual sign of the inclination vector. To estimate whether the choice of the sign of *I* makes a difference in the outcome of the analysis, igneous rock data with MV ≥ 3 were selected. Entries with mixed polarity were neglected. The set of 903 records was reduced to normal (*N* = 545) and reversed (*N* = 358) subsets according to inclination, as seen in Table 3. As seen in Fig. 8, positive inclinations have a distribution close to the GAD, whereas the negative ones do not follow any clearly defined zonal harmonic decomposition. The difference between positive- and negative-polarity populations is most likely due to the fact that Laurentia and Baltica, the two most extensively studied cratons, occupied shallow northerly latitudes for most of the Paleo- and Mesoproterozoic (Pesonen et al., 2012b). In our data, these are characterized by positive inclinations with just a few exceptions, thus supporting the hypothesis of long stable-polarity intervals in the Precambrian (Elston et al., 2002).

Table 3
Inclination distributions for data with different Van der Voo gradings. Igneous and metamorphic rocks only, cratonic binning not applied. Normal and reversed polarities combined in polarity pairs whenever reasonable. The values of the test statistic X^2 calculated using GAD as a null hypothesis. The distribution with MV = 6 is so small that χ^2 testing cannot be properly applied. See also Figure 8.

Interval	MV ≥ 1	MV ≥ 2	MV ≥ 3	GAD (*N* = 999)
$0 \leq \|I\| < 10°$	204 (11.2%)	172 (11.1%)	114 (11.6%)	87 (8.8%)
$10 \leq \|I\| < 20°$	196 (10.8%)	158 (10.6%)	109 (11.0%)	90 (9.1%)
$20 \leq \|I\| < 30°$	202 (11.1%)	165 (10.8%)	100 (10.1%)	96 (9.7%)
$30 \leq \|I\| < 40°$	241 (13.3%)	193 (12.5%)	115 (11.7%)	108 (10.9%)
$40 \leq \|I\| < 50°$	278 (15.3%)	228 (15.3%)	147 (14.9%)	124 (12.6%)
$50 \leq \|I\| < 60°$	232 (12.8%)	191 (12.8%)	116 (11.8%)	140 (14.2%)
$60 \leq \|I\| < 70°$	216 (11.9%)	194 (12.4%)	132 (13.4%)	152 (15.4%)
$70 \leq \|I\| < 80°$	169 (9.3%)	154 (10.5%)	105 (10.6%)	132 (13.4%)
$80 \leq \|I\| < 90°$	76 (4.2%)	67 (4.3%)	49 (5.0%)	58 (5.9%)
Combined	1814 (100%)	1522 (100%)	987 (100%)	987
X^2	89.790	54.614	30.942	–
p-Value	<0.0001	<0.0001	0.0001	–

Interval	MV ≥ 4	MV ≥ 5	MV = 6
$0 \leq \|I\| < 10°$	56 (11.6%)	22 (12.3%)	3 (7.7%)
$10 \leq \|I\| < 20°$	53 (11.0%)	23 (12.8%)	6 (15.4%)
$20 \leq \|I\| < 30°$	40 (8.3%)	15 (8.4%)	2 (5.1%)
$30 \leq \|I\| < 40°$	51 (10.6%)	23 (12.8%)	2 (5.1%)
$40 \leq \|I\| < 50°$	72 (14.9%)	22 (12.3%)	8 (20.5%)
$50 \leq \|I\| < 60°$	59 (12.2%)	20 (11.2%)	5 (12.8%)
$60 \leq \|I\| < 70°$	74 (15.3%)	30 (16.8%)	6 (15.4%)
$70 \leq \|I\| < 80°$	55 (11.4%)	13 (7.3%)	4 (10.3%)
$80 \leq \|I\| < 90°$	23 (4.8%)	11 (6.1%)	3 (7.7%)
Combined	483 (100%)	179 (100%)	39
X^2	13.038	14.404	–
p-Value	0.111	0.072	–

Table 4
Global distributions for binned ($N = 233$) and unbinned ($N = 483$) crystalline rock data (MV ≥ 4), along with the reduced-size unbinned distribution. The reduced-size unbinned data has been selected randomly from the filtered, unbinned dataset and demonstrates how the size of the distribution affects the chi-square values. The values of the test statistic X^2 have been calculated for all distributions with GAD as a null hypothesis. For comparison, the distribution calculated from the unfiltered, unbinned raw data (i.e. our entire database, including sedimentary records) is also shown. Unbinned and binned distributions are plotted in Fig. 9, along with the best-fit model of the Precambrian.

Interval	Filtered, unbinned	Filtered, binned	Filtered, unbinned, reduced size	Unfiltered, unbinned
$0 \le \lvert I \rvert < 10^\circ$	56 (11.6%)	27 (11.6%)	27 (11.6%)	449 (13.8%)
$10 \le \lvert I \rvert < 20^\circ$	53 (11.0%)	25 (10.7%)	26 (11.2%)	395 (12.2%)
$20 \le \lvert I \rvert < 30^\circ$	40 (8.3%)	21 (9.0%)	19 (8.2%)	412 (12.7%)
$30 \le \lvert I \rvert < 40^\circ$	51 (10.6%)	28 (12.0%)	25 (10.7%)	480 (14.8%)
$40 \le \lvert I \rvert < 50^\circ$	72 (14.9%)	36 (15.5%)	35 (15.0%)	464 (14.3%)
$50 \le \lvert I \rvert < 60^\circ$	59 (12.2%)	32 (13.7%)	28 (12.0%)	386 (11.9%)
$60 \le \lvert I \rvert < 70^\circ$	74 (15.3%)	29 (12.4%)	36 (15.5%)	317 (9.8%)
$70 \le \lvert I \rvert < 80^\circ$	55 (11.4%)	24 (10.3%)	26 (11.2%)	246 (7.6%)
$80 \le \lvert I \rvert < 90^\circ$	23 (4.8%)	11 (4.7%)	11 (4.7%)	97 (3.0%)
Combined	483 (100%)	233 (100%)	233 (100%)	3246 (100%)
X^2	13.038	9.210	7.699	411.765
p-Value	0.111	0.325	0.4433	<0.0001

The concentration of steep negative inclinations, contrasted with shallow positive ones, has been observed in the data of the late Mesoproterozoic Lake Superior region (e.g. Pesonen, 1979; Green et al., 1987; Tauxe and Kodama, 2009). This phenomenon, although visible in Fig. 8, is most likely not a manifestation of any long-lived feature of the geomagnetic field, since the temporal distributions of N and R data do not overlap, but rather, N records are systematically younger than R ones. The difference between the positive- and negative-inclination curves is most likely due to the fact that Fennoscandia (Baltica), and Laurentia, the most widely studied Precambrian continents, had a vast majority of positive inclinations, many of them from 1.8 to 1.2 Ma when the continents most likely drifted together (Evans and Pisarevsky, 2008; Salminen et al., 2009; Pisarevsky and Bylund, 2010). Also the North and South China blocks have a majority of positive inclinations.

Since no detailed APW paths are available for any craton throughout the Precambrian and models of the configuration of continents are tentative at best, observations about positive and negative values of inclination tell nothing about the actual polarities of the geomagnetic field. Comprehensive time sequences available for comparison between polarities observed in different cratons are limited, although the correlation of Laurentia and Baltica between 1.88 Ga and 1.02 Ga is possible. Their common history is demonstrated by paleolatitude curves, similar APW paths and repeatedly similar positions in paleomagnetically generated reconstructions (Pesonen et al., 2012b). Some Precambrian time slots are, however, strongly over- and other underrepresented in the number of observations. This is mainly due to the fact that magmatic activity generally occurs in pulses, which generate large igneous provinces (LIPs) (Ernst and Buchan, 2002). One of the most remarkable ones is the rifting of Keweenawan 1.12–1.06 Ma ago, which accounts for plenty of paleomagnetic results, not only in Laurentia but also in Antarctica (Coats Land nunataks, Gose et al., 1997), Baltica (Salla diabase dykes, Salminen et al., 2009) and South Africa (Umkondo LIP, Gose et al., 2006).

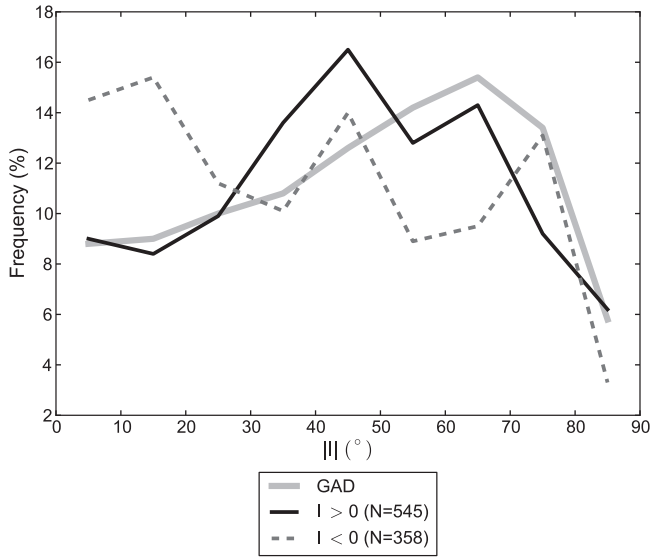

Fig. 8. Comparison of positive (+) and negative (−) inclinations according to data in Table 1. The group of positive inclinations behaves almost like GAD. The distribution of negative inclinations is highly irregular, and a concentration of low inclinations is visible.

3.3. Age

The influence of the geologic age was studied by sorting observations from igneous and metamorphic rocks into four time windows according to geological eras: Archean (>2500 Ma), Paleoproterozoic (2500...1600 Ma), Mesoproterozoic (1600...1000 Ma) and Neoproterozoic (1000...542 Ma). In this age analysis, sedimentary data were dropped out since there were virtually no high-quality paleomagnetic studies on sediments older than 2500 Ma. Even in the case of crystalline rocks, the functionality of statistical testing for Archean data is weak due to the small number of entries and their strong concentration in Kalahari (Africa) and Pilbara (Australia). Distributions for igneous and metamorphic rocks of varying ages are shown in Fig. 7 and Table 2. Mesoproterozoic data appear to be biased towards low inclinations, whereas the other time windows are more similar to GAD. Because a large part of the Mesoproterozoic interval is dominated by the existence of the supercontinent Nuna, which occupied low to moderate paleolatitudes between 1600 and ~1300 Ma (Zhang et al., 2012), the low-latitude bias of Mesoproterozoic data is not surprising. The general concordance of other time intervals with the GAD model is perhaps unexpected, because those durations (less than 500 million years for the Neoproterozoic, in particular) have been considered generally insufficient for continents to sample the Earth's surface adequately (Meert et al., 2003).

3.4. Quality filtering

Successive quality filtering alters the database inclination distributions, at first moderately, and then substantially (Fig. 9). In this test, crystalline rocks only are included. As high-pass filters progress through MV values as high as 3–4, the low-inclination bias decreases slightly, such that the data curves become coincident with the GAD curve at 20–40° inclination values. In these

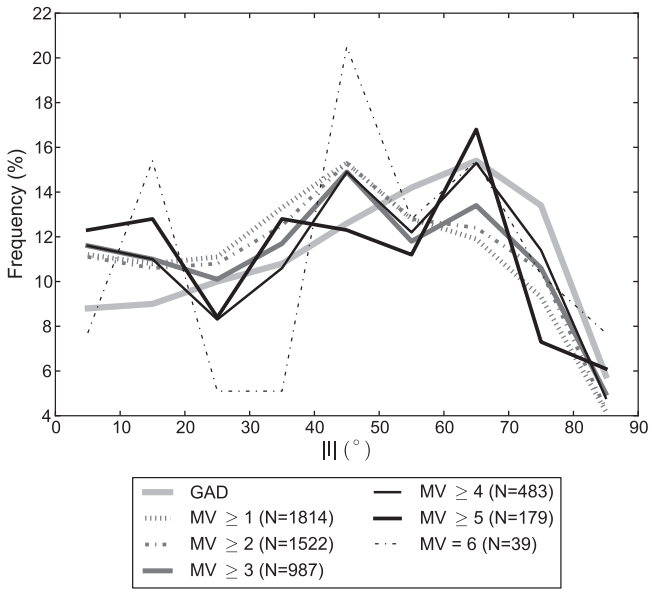

Fig. 9. The effect of quality filtering in inclination distributions. Data with MV (Modified Van der Voo gradings) from Table 3, with igneous and metamorphic rocks. All other distributions, except that of MV = 6, are statistically significant.

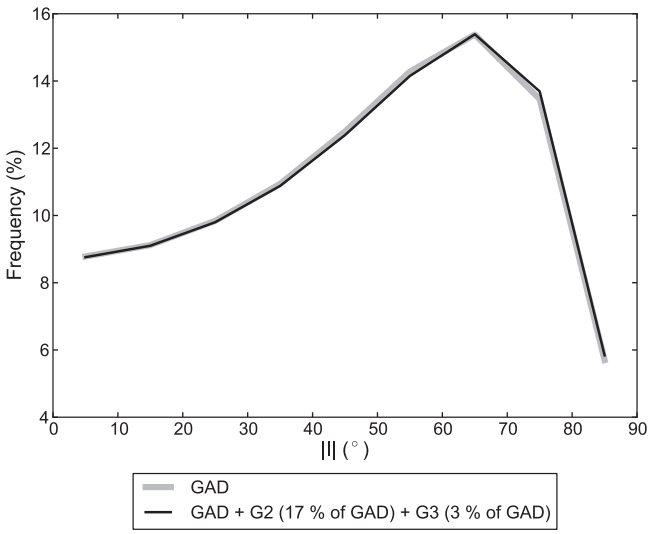

Fig. 10. The non-uniqueness of inclination distributions. A certain superposition of quadrupolar and octupolar fields, combined with the GAD, is a source to a distribution equal in appearance to that generated by the GAD only.

examples, there remains an anomalously large frequency of 0–20° values, and a frequency peak at 40–50° rather than the 60–70° peak predicted by GAD. Nonetheless, successive filtering through these stages substantially decreases the chi-squared statistic (Table 3), even though the deviation from GAD is slightly larger in MV ≥ 5 dataset when compared to MV ≥ 4. At the highest level of quality filtering (MV = 6), the statistics of small data create jagged frequency curves and render the chi-square test meaningless.

As noted above, filtering to MV ≥ 3 or MV ≥ 4 appears to be the best compromise between quality control and a statistically large enough dataset for analysis. With MV ≥ 3 on unbinned igneous and metamorphic rock data, the optimal field model has G2 = 0% and G3 = 6% of GAD. With MV ≥ 4, also on unbinned igneous and metamorphic rocks only, two equally plausible best-fit models exist: one with G2 = 1% and G3 = 4%, and another with G2 = 7% and G3 = 6%. With binned igneous and metamorphic rock data filtered by MV ≥ 4, the best fit has G2 = 0% and G3 = 6%. As a compromise, we ended up using values of G2 = 2% and G3 = 5% of GAD, acknowledging the possibility that our binning procedure may cause slight bias towards mid-inclination values (Table 4).

4. Discussion

The new results suggest that the optimal geomagnetic field model of the Precambrian, according to the database-wide inclination test, is not far from the field predicted by the GAD model. This is in strong contrast to all previous studies (Piper and Grant, 1989; Kent and Smethurst, 1998; Tauxe and Kodama, 2009), where distinct low-inclination biases were observed. The new analysis supports the existence of a small octupolar (ca. 0–8% of GAD) component. The quadrupole can also be 0–10% of GAD, although the distribution is much more sensitive to small changes in G3 rather than in G2. Models with G3 > 0.12 are mostly incompatible with the observed data, though their functionality is improved when they include a small G2 term, too. Not surprisingly, the deviation from the GAD is smallest for the highest-quality observations, including so-called key poles (Buchan et al., 2000). They have well-defined isotopic ages, small statistical error parameters, and their primary remanent magnetization has been properly isolated.

Our results thus remove an inconsistency between earlier database-wide inclination tests that suggested substantial non-dipolar components of the field (notably, Kent and Smethurst, 1998), versus the comparison of Precambrian evaporite paleolatitudes with modern Hadley circulation (Evans, 2006), which gave results indistinguishable from the GAD model. In the latter study, the optimal value of G3 for pre-Ediacaran data, all other factors held constant, was 13%, with large uncertainties enveloping GAD but barely excluding the earlier-proposed 25% value. By reducing the inclination test anomaly from G3 ~25% to G3 ~5%, our present study lessens the need for geophysical speculations on a very late growth of the inner core (Kent and Smethurst, 1998), or models of particular heat-flow patterns across the core–mantle boundary (Bloxham, 2000). Such effects might have existed at various stages of the Precambrian, and could account for the nonzero G3 in our optimally filtered data subset, but they are not needed to be as large as previously thought. In addition, the assumption that continents have sampled all latitudes adequately during their drift history, although debated (Meert et al., 2003; McFadden, 2004; Evans, 2005; Evans and Hoye, 2007) cannot cause a serious mismatch between the GAD model and observations. It is also evident that certain sources of data, such as redbeds, coral reefs, evaporites, shungites or other rocks known to deposit at shallow to moderate latitudes (Evans et al., 1997; Pesonen et al., 2003) should not be given a strong weight in evaluating the validity of the GAD hypothesis.

5. Conclusions

Even though our inclination analysis suggests the validity of the GAD hypothesis during the Precambrian, the method used for the analysis is by definition non-unique. For example, a combination of a moderate quadrupole (17% of GAD) and a very small octupole (3% of GAD) produces an inclination distribution, which appears identical to that generated by g_1^0 only (Fig. 10). Hence other methods, such as the paleosecular variation analysis (Smirnov et al., 2011) and asymmetries of the field reversals (Veikkolainen et al., 2013a) should be used to find the best model for the geomagnetic field of the Precambrian. The conclusion that the presence of a small octupolar field causes a larger discrepancy in the predicted paleolatitudes of continents, than a small quadrupole does, has formerly been used in improving the reconstruction of the Pangaea supercontinent (Van der Voo and Torsvik, 2001). The relatively

small number of high-latitude paleomagnetic poles was originally explained by the rejection of suspected steep directions as representing the present-day geomagnetic field (Lapointe et al., 1978). This theory is no longer trustworthy, particularly due to the fact that it was based on North American data, and the current database (Pesonen et al., 2012a) contains nearly 1000 moderate- or high-quality (MV ≥ 3) results where the exclusion of the present-day field (PEF) has been generally done in a correct way. Although the so-called PEF contamination is still relevant and must be carefully documented, it is not the dominant explanation for steep (high-latitude) remanence directions.

When only unaltered, most reliable observations of inclination are considered, the support for the GAD hypothesis is remarkable. Therefore it is reasonable to assume that the geodynamo of the far past is driven by mostly the same processes that have generated the field of the most recent geological eras.

Acknowledgements

The completion of this work owes much to all researchers, who have participated in our paleomagnetic database project, especially Dr. Satu Mertanen from Geological Survey of Finland, Prof. Sten-Åke Elming from Luleå University of Technology, Prof. Joseph Meert from University of Florida, Dr. Phillip Schmidt from CSIRO Earth Science & Resource Engineering, Dr. Sergei Pisarevsky from University of Western Australia, and research assistants at University of Helsinki. Also the financial support from University of Helsinki, and Oskar Öflund foundation is highly appreciated. We appreciate the critical reviews by Rob van der Voo and an anonymous reviewer. This paper is an output of the 6th Nordic Paleomagnetic Workshop, held in Luleå, Sweden, September 15th to 22nd, 2009.

Appendix A. Supplementary data

Supplementary data associated with this article can be found, in the online version, at http://dx.doi.org/10.1016/j.precamres.2013.09.004.

References

Bates, M.P., Jones, D.L., 1996. A palaeomagnetic investigation of the Mashonaland dolerites, north-east Zimbabwe. Geophysical Journal International 126, 513–524.
Biggin, A.J., Strik, G.H.M.A., Langereis, C.G., 2008. Evidence for a very-long-term trend in geomagnetic secular variation. Nature Geoscience 1, 395–398.
Bingham, D.K., Evans, M.E., 1976. Paleomagnetism of the Great Slave Supergroup, Northwest Territories, Canada: the Stark Formation. Canadian Journal of Earth Science 13, 563–578.
Bloxham, J., 2000. Sensitivity of the geomagnetic axial dipole to thermal core–mantle interactions. Nature 405, 63–65.
Buchan, K.L., LeCheminant, A.N., van Breemen, O., 2009. Paleomagnetism and U–Pb geochronology of the Lac de Gras diabase dyke swarm, Slave Province, Canada: implications for relative drift of Slave and Superior provinces in the Paleoproterozoic. Canadian Journal of Earth Sciences 46, 361–379.
Buchan, K.L., Mertanen, S., Park, R.G., Pesonen, L.J., Elming, S.-Å., Abrahamsen, N., Bylund, G., 2000. Comparing the drift of Laurentia and Baltica in the Proterozoic: the importance of key paleomagnetic poles. Tectonophysics 319, 167–198.
Carlut, J., Courtillot, V., 1998. How complex is the time-averaged geomagnetic field over the past 5 million years? Geophysical Journal International 134, 527–554.
Cogné, J.P., Halim, N., Chen, Y., Courtillot, V., 1999. Resolving the problem of shallow magnetizations of Tertiary age in Asia: insights from paleomagnetic data from the Qiangtang, Kunlun, and Qaidam blocks (Tibet, China), and a new hypothesis. Journal of Geophysical Research: Solid Earth 104, 17715–17734.
Courtillot, V., Besse, J., 2004. A long-term octupolar component in the geomagnetic field? (0–200 million years B.P). In: Channell, J.E.T., Kent, D.V., Lowrie, W., Meert, J.G. (Eds.), Timescales of the Paleomagnetic Field, Geophysical Monograph, vol. 145. American Geophysical Union, Washington DC, pp. 59–74.
Donadini, F., Pesonen, L.J., Korhonen, K., Deutsch, A., Harlan, S.S., 2011. Paleomagnetism and paleointensity of the 1.1 Ga old diabase sheets from Central Arizona. Geophysica 47, 3–30.
Donadini, F., Pesonen, L.J., Korhonen, K., Deutsch, A., Harlan, S.S., Heaman, L.M., 2012. Symmetric and asymmetric reversals in the 1.1 Ga Central Arizona diabases: the debate continues. In: Mertanen, S., Pesonen, L.J., Sangchan, P. (Eds.), Supercontinent Symposium 2012. Programme and Abstracts. , pp. 35–36.
Donadini, F., Riisager, P., Korhonen, K., Kahma, K., Pesonen, L., Snowball, I., 2007. Holocene geomagnetic paleointensities: a blind test of absolute paleointensity techniques and materials. Physics of the Earth and Planetary Interiors 161, 19–35.
Elston, D.P., Enkin, R.J., Baker, J., Kisilevsky, D.K., 2002. Tightening the belt: paleomagnetic-stratigraphic constraints on deposition, correlation, and deformation of the Middle Proterozoic (ca. 1.4 Ga) Belt-Purcell Supergroup, United States and Canada. Geological Society of America Bulletin 114, 619–638.
Ernst, R.E., Buchan, K.L., 1993. Paleomagnetism of the Abitibi dyke swarm, southern Superior Province, and implications for the Logan Loop. Canadian Journal of Earth Sciences 30, 1886–1897.
Ernst, R.E., Buchan, K.L., 2002. Maximum size and distribution in time and space of mantle plumes: evidence from large igneous provinces. Journal of Geodynamics 34, 309–342.
Evans, D.A.D., 1998. True polar wander, a supercontinental legacy. Earth and Planetary Science Letters 157, 1–8.
Evans, D.A.D., 2003. A fundamental Precambrian–Phanerozoic shift in Earth's glacial style? Tectonophysics 375, 353–385.
Evans, D.A.D., 2006. Proterozoic low orbital obliquity and axial-dipolar geomagnetic field from evaporite palaeolatitudes. Nature 444, 51–55.
Evans, D.A.D., Beukes, N.J., Kirschvink, J.L., 1997. Low-latitude glaciation in the Palaeoproterozoic era. Nature 386, 262–266.
Evans, D.A.D., Pisarevsky, S.A., 2008. Plate tectonics on early Earth? Weighing the paleomagnetic evidence. In: Condie, K., Pease, V. (Eds.), When Did Plate Tectonics Begin? Geological Society of America Special Paper 440. , pp. 249–263.
Evans, M.E., 1976. Test of the dipolar nature of the geomagnetic field throughout Phanerozoic time. Nature 262, 676–677.
Evans, M.E., 2005. Testing the geomagnetic dipole hypothesis: paleolatitudes sampled by large continents. Geophysical Journal International 161, 266–267.
Evans, M.E., Hoye, G.S., 2007. Testing the GAD throughout geological time. Earth Planets Space 59, 697–701.
Gose, W.A., Helper, M.A., Connelly, J.N., Hutson, F.E., Dalziel, I.W.D., 1997. Paleomagnetic data and U–Pb isotopic age determinations from Coats Land, Antarctica: implications for late Proterozoic plate reconstructions. Journal of Geophysical Research: Solid Earth 102, 7887–7902.
Gose, W.A., Hanson, R.E., Dalziel, I.W.D., Pancake, J.A., Seidel, E.K., 2006. Paleomagnetism of the 1.1 Ga Umkondo large igneous province in southern Africa. Journal of Geophysical Research: Solid Earth 111, B09101.
Green, J.C., Bornhorst, T.J., Chandler, V.W., Mudrey Jr., M.G., Myers, P.E., Pesonen, L.J., Wilband, J.T., 1987. Keweenawan Dykes of the Lake Superior Region: evidence for evolution of the middle Proterozoic. In: Halls, H.C., Fahrig, W.F. (Eds.), Mafic Dyke Swarms, Geological Association of Canada Special Paper. , pp. 289–302.
Grower, M., 2005. Closing Pandora's Box: additional insights on inclination bias using a random walk approach. Journal of Undergraduate Research, University of Florida 6 (6), 16.
Halls, H.C., Davis, D.W., 2004. Paleomagnetism and U–Pb geochronology of the 2.17 Ga Biscotasing dyke swarm, Ontario, Canada: evidence for vertical-axis crustal rotation across the Kapuskasing Zone. Canadian Journal of Earth Sciences 41, 255–269.
Halls, H.C., Palmer, H.C., 1990. The tectonic relationship of two Early Proterozoic dyke swarms to the Kapuskasing Structural Zone: a paleomagnetic and petrographic study. Canadian Journal of Earth Sciences 27, 87–103.
Hatakeyama, T., Kono, M., 2002. Geomagnetic field models for the last 5 myr: time-averaged field and secular variation. Physics of the Earth and Planetary Interiors 133, 181–201.
Irving, E., Davidson, A., McGlynn, J.C., 1984. Paleomagnetism of gabbros of the Early Proterozoic Blachford Lake intrusive suite and Easter Island dyke, Great Slave Lake, NWT: possible evidence for the earliest continental drift. Geophysical Surveys 7, 1–25.
Kent, D.V., Smethurst, M.A., 1998. Shallow bias of paleomagnetic inclinations in the Paleozoic and Precambrian. Earth and Planetary Science Letters 160, 391–402.
Khramov, A.N., Iosifidi, A.G., 2012. Asymmetry of geomagnetic polarity: equatorial dipole, Pangaea and the earth's core. Izvestiya, Physics of the Solid Earth 48, 28–41.
King, R.F., 1955. The remanent magnetism of artificially deposited sediments. Monthly Notices of the Royal Astronomical Society, Geophysical Supplement 7, 115–134.
Kodama, K., 2012. Paleomagnetism of Sedimentary Rocks: Process and Interpretation. Wiley-Blackwell, Chichester, 164 pp.
Komissarova, R.A., Iosifidi, A.G., Khramov, A.N., 1997. Geomagnetic reversals recorded in the Late Riphean Katav Formation, South Urals. Izvestiya, Physics of the Solid Earth 33, 139–146.
Lapointe, P.L., Roy, J.L., Morris, W.A., 1978. What happened to the high-latitude paleomagnetic poles? Nature 273, 655–657.
Livermore, R.A., Vine, F.J., Smith, A.G., 1984. Plate motions and the geomagnetic field. II. Jurassic to Tertiary. Geophysical Journal of the Royal Astronomical Society 79, 939–961.
McElhinny, M.W., 2004. Geocentric axial dipole hypothesis: a least squares perspective. In: Channell, J.E.T., Kent, D.V., Lowrie, W., Meert, J.G. (Eds.), Timescales of the Paleomagnetic Field, Geophysical Monograph, vol. 145. American Geophysical Union, Washington DC, pp. 1–12.
McElhinny, M.W., Lock, J., 1996. IAGA paleomagnetic databases with access. Surveys in Geophysics 17, 575–591.

McFadden, P.L., 2004. Is 600 Myr long enough for the random palaeogeographic test of the geomagnetic axial dipole assumption? Geophysical Journal International 158, 443–445.
Meert, J.G., Tamrat, E., Spearman, J., 2003. Non-dipole fields and inclination bias: insights from a random walk analysis. Earth and Planetary Science Letters 214, 395–408.
Merrill, R.T., McElhinny, M.W., McFadden, P.L., 1998. The Magnetic Field of the Earth. Paleomagnetism, The Core and the Deep Mantle. Academic Press, San Diego, pp. 531pp.
Nevanlinna, H., Pesonen, L.J., 1983. Late Precambrian Keweenawan asymmetric polarities as analyzed by axial offset dipole geomagnetic models. Journal of Geophysical Research: Solid Earth 88, 645–658.
Pesonen, L.J., 1979. Paleomagnetism of Late Precambrian Keweenawan igneous and baked contact rocks from Thunder Bay district, northern Lake Superior. Bulletin of the Geological Society of Finland 51, 27–44.
Pesonen, L.J., Elming, S.-Å., Mertanen, S., Pisarevsky, S., D'Agrella-Filho, M.S., Meert, J.G., Schmidt, P.W., Abrahamsen, N., Bylund, G., 2003. Paleomagnetic configuration of continents during the Proterozoic. Tectonophysics 375, 289–324.
Pesonen, L., Evans, D.A.D., Veikkolainen, T., Sangchan, P., 2012a. A novel Precambrian paleomagnetic database: the basis for analysing supercontinents, GAD and PSV. In: Mertanen, S., Pesonen, L.J., Sangchan, P. (Eds.), Supercontinent Symposium 2012. Programme and Abstracts. , pp. 104–105.
Pesonen, L.J., Mertanen, S., Veikkolainen, T., 2012b. Paleo-Mesoproterozoic supercontinents – a paleomagnetic view. Geophysica 48, 5–47.
Piper, J.D.A., Grant, S., 1989. A paleomagnetic test of the axial dipole assumption and implications for continental distributions through geological time. Physics of the Earth and Planetary Interiors 55, 37–53.
Pisarevsky, S.A., 2005. New edition of the global paleomagnetic database. EOS Transactions, American Geophysical Union 86, 170.
Pisarevsky, S.A., Bylund, G., 2006. Palaeomagnetism of 935 Ma mafic dykes in southern Sweden and implications for the Sveconorwegian Loop. Geophysical Journal International 166, 1095–1104.
Pisarevsky, S.A., Bylund, G., 2010. Paleomagnetism of 1780–1770 Ma mafic and composite intrusions of Småland (Sweden): implications for the Mesoproterozoic supercontinent. American Journal of Science 310, 1168–1186.
Salminen, J., Pesonen, L.J., Mertanen, S., Vuollo, J., Airo, M.-L., 2009. Palaeomagnetism of the Salla Diabase Dyke, northeastern Finland and its implication to the Baltica – Laurentia entity during the Mesoproterozoic. Geological Society, London, Special Publications 323, 199–217.
Schmidt, P.E., Williams, G.E., 2010. Ediacaran palaeomagnetism and apparent polar wander path for Australia: no large true polar wander. Geophysical Journal International 182, 711–726.
Schmidt, P.W., Williams, G.E., Embleton, B.J.J., 1991. Low paleolatitude of Late Proterozoic glaciation: early timing of remanence of haematite in the Elatina formation, South Australia. Earth and Planetary Science Letters 105, 355–367.
Schmidt, P.E., Williams, G.E., McWilliams, M.O., 2009. Paleomagnetism and magnetic anisotropy of late Neoproterozoic strata, South Australia: implications for the palaeolatitude of late Cryogenian glaciation, cap carbonate and the Ediacaran System. Precambrian Research 174, 35–52.
Smirnov, A.V., Tarduno, J.A., Evans, D.A.D., 2011. Evolving core conditions ca. 2 billion years ago detected by paleosecular variation. Physics of the Earth and Planetary Interiors 187, 225–231.
Swanson-Hysell, N.L., Maloof, A.C., Weiss, B.P., Evans, D.A.D., 2009. No asymmetry in geomagnetic reversals recorded by 1.1-billion-year-old Keweenawan basalts. Nature Geoscience 2, 713–717.
Tauxe, L., Kent, D.V., 2004. A simplified statistical model for the geomagnetic field and the detection of shallow bias in paleomagnetic inclinations: was the ancient magnetic field dipolar? In: Channell, J.E.T., Kent, D.V., Lowrie, W., Meert, J.G. (Eds.), Timescales of the Paleomagnetic Field, Geophysical Monograph, vol. 145. American Geophysical Union, Washington DC, pp. 101–115.
Tauxe, L., Kodama, K.P., 2009. Paleosecular variation models for ancient times: clues from Keweenawan lava flows. Physics of the Earth and Planetary Interiors 177, 31–45.
Torsvik, T.H., Van der Voo, R., Preeden, U., Mac Niocaill, C., Steinberger, B., Doubrovine, P.V., van Hinsbergen, D.J.J., Domeier, M., Gaina, C., Tohver, E., Meert, J.G., McCausland, P.J.A., Cocks, L.R.M., 2012. Phanerozoic polar wander, palaeogeography and dynamics. Earth Science Reviews 114, 325–368.
Van der Voo, R., 1990. The reliability of paleomagnetic data. Tectonophysics 184, 1–9.
Van der Voo, R., Torsvik, T.H., 2001. Evidence for Permian and Mesozoic non-dipole fields provides an explanation for Pangea reconstruction problems. Earth and Planetary Science Letters 187, 71–81.
Veikkolainen, T., Pesonen, L., Korhonen, K., 2013a. An analysis of geomagnetic field reversals supports the validity of the Geocentric Axial Dipole (GAD) hypothesis in the Precambrian. Precambrian Research (in this issue).
Veikkolainen, T., Pesonen, L.J., Evans, D.A.D., 2013b. PALEOMAGIA, a PHP/MYSQL database of Precambrian paleomagnetic data. Geochemistry Geophysics Geosystems (in preparation).
Veselovskiy, R.V., Pavlov, V.E., 2006. New paleomagnetic data for the Permian-Triassic Trap rocks of Siberia and the problem of a non-dipole geomagnetic field at the Paleozoic–Mesozoic boundary. Russian Journal of Earth Sciences 8, ES1002.
Wegener, A., 1929. Die Entstehung der Kontinente und Ozeane. Friedrich Vieweg & Sohn Aktien Gesellschaft, Braunschweig.
Zhang, S., Li, Z.-X., Evans, D.A.D., Wu, H., Li, H., Dong, J., 2012. Pre-Rodinia supercontinent Nuna shaping up: a global synthesis with new paleomagnetic results from North China. Earth and Planetary Science Letters 353-354, 145–155.

Supplementary tables

These tables show the values of chi-square test statistic (X^2) in the statistical modelling where different superpositions of GAD+G2+G3 are set as null hypotheses. The values of the axial quadrupole (G2), ranging from 0 % to 10 % of the strength of GAD, are shown by the column numbers of the table, whereas the row numbers indicate the value of the axial octupole (G3), ranging from 0 % to the 25 % of the strength of GAD. The values of X^2 not exceeding the critical value 15.507 are emphasized with underlined font, meaning that the corresponding zonal field model passes the χ^2 test. Values with italic underlined font values point to the minima of X^2, referring to the best-fit zonal field models in each three sets of observations.

1. Unbinned, MV ≥ 4, crystalline rocks (igneous and) metamorphic)

0.25	100.8	100.9	98.66	98.51	99.49	96.44	95.85	96.03	96.30	95.96	97.01
0.24	91.58	91.83	90.13	91.73	91.43	89.28	88.51	88.99	87.58	86.99	86.81
0.23	83.50	84.46	82.80	83.00	82.71	81.61	82.89	79.84	80.12	80.05	78.07
0.22	76.78	76.53	76.17	76.01	74.07	74.16	75.29	73.16	72.44	71.69	72.46
0.21	69.15	68.43	69.99	69.13	68.17	67.70	66.94	66.53	65.20	64.90	63.52
0.20	62.84	61.94	62.17	62.17	61.94	60.69	59.95	59.74	58.86	58.69	57.56
0.19	58.18	55.75	55.66	55.45	55.06	53.90	54.71	52.88	51.76	52.90	51.55
0.18	48.54	50.26	49.18	50.05	48.82	49.04	48.79	47.13	46.90	46.58	44.99
0.17	44.63	42.51	44.05	43.23	43.80	42.86	42.50	41.97	41.80	40.89	39.94
0.16	39.75	39.25	38.36	38.87	39.01	37.29	36.96	36.83	35.83	35.58	34.23
0.15	34.16	34.21	34.52	33.66	33.00	34.02	32.52	32.55	31.67	30.62	29.92
0.14	29.41	29.50	29.87	27.98	29.59	28.69	28.41	27.71	27.87	26.31	29.92
0.13	26.66	26.68	24.82	25.91	25.12	24.89	24.79	24.36	24.07	22.82	22.37
0.12	20.88	21.82	23.01	21.47	22.13	22.31	20.90	20.64	20.23	20.28	18.80
0.11	18.47	18.62	19.84	19.68	18.73	17.92	18.60	17.58	17.32	16.30	16.38
0.10	15.92	16.48	16.46	16.86	16.12	15.22	15.61	14.99	14.90	14.15	14.56
0.09	12.57	13.63	13.09	13.48	13.61	14.52	13.06	12.68	13.23	12.97	12.17
0.08	11.65	11.71	11.97	11.84	12.13	12.36	11.09	11.62	11.51	11.08	11.73
0.07	11.16	10.24	10.40	10.40	10.59	10.66	10.22	10.38	10.92	9.36	9.30
0.06	10.15	9.99	9.90	9.56	8.83	10.05	10.01	**8.33**	9.13	10.04	9.06
0.05	8.88	9.27	8.83	9.38	8.43	8.43	8.62	9.86	9.66	9.40	9.71
0.04	9.30	**8.33**	8.93	9.06	9.27	9.47	9.96	9.05	9.30	9.12	9.41
0.03	9.79	9.68	9.23	9.12	9.41	9.85	10.46	9.49	10.10	9.44	10.42
0.02	11.32	11.09	11.05	9.83	10.63	11.31	11.22	11.17	11.33	12.41	11.80
0.01	12.28	12.18	12.60	11.91	11.80	12.31	12.52	12.49	12.99	14.51	13.58
0.00	13.04	14.09	14.49	13.76	14.25	14.04	14.77	14.42	15.48	16.87	16.32
G3/G2	**0.00**	**0.01**	**0.02**	**0.03**	**0.04**	**0.05**	**0.06**	**0.07**	**0.08**	**0.09**	**0.10**

2. Binned, MV ≥ 4, crystalline rocks

0.25	36.58	35.99	36.16	35.96	35.12	35.10	34.13	33.78	34.20	32.93	31.93
0.24	33.28	32.51	32.44	31.90	31.09	31.95	30.86	28.93	29.79	28.84	28.43
0.23	30.82	29.74	29.72	28.50	27.74	27.86	27.08	27.51	26.38	25.58	25.42
0.22	25.64	25.35	26.00	25.58	24.92	24.55	24.11	24.57	23.93	23.97	23.29
0.21	21.98	22.68	22.01	22.02	23.08	21.64	21.99	21.76	21.15	20.45	19.57
0.20	19.92	20.77	19.98	20.18	19.65	18.49	19.07	18.97	17.96	17.23	16.83
0.19	18.37	18.08	17.32	17.11	16.92	16.59	16.01	15.40	14.72	14.86	14.23
0.18	15.19	14.98	13.86	15.06	14.08	14.26	14.76	13.88	12.53	11.80	11.24
0.17	13.13	12.03	12.41	12.00	11.82	11.47	11.64	11.14	11.13	10.67	10.42
0.16	10.99	10.93	10.17	10.15	9.77	9.46	9.76	9.50	8.95	8.30	8.52
0.15	8.48	8.03	8.49	9.41	8.76	8.95	7.76	6.84	7.20	6.61	7.32
0.14	7.05	7.15	7.35	6.54	6.48	6.12	6.55	6.52	6.73	5.39	5.36
0.13	5.34	5.86	6.15	5.84	5.83	5.18	5.03	4.78	4.46	5.39	4.89
0.12	4.75	5.23	4.81	4.80	4.65	4.82	4.80	4.23	4.07	3.83	3.75
0.11	4.91	4.02	4.04	4.02	4.33	3.90	3.17	3.62	3.94	2.84	3.46
0.10	2.75	3.59	4.17	3.73	3.15	2.84	3.15	2.80	3.12	3.26	3.21
0.09	2.89	3.17	2.80	3.12	3.34	2.88	2.88	2.94	3.03	2.92	3.41
0.08	2.88	2.83	2.33	2.92	2.80	2.67	2.99	2.71	3.42	3.18	3.10
0.07	2.70	2.69	2.63	2.70	2.70	2.81	3.75	3.29	3.50	3.40	3.62
0.06	**2.27**	2.29	2.75	2.75	2.61	2.92	3.00	3.61	3.90	3.65	3.08
0.05	3.83	3.76	3.31	3.98	3.68	3.28	3.43	3.23	4.16	4.37	3.82
0.04	4.42	4.06	4.69	4.69	4.79	4.46	4.89	4.38	4.53	5.06	4.59
0.03	5.21	5.51	5.54	5.38	5.52	5.44	5.62	4.82	4.68	5.94	5.76
0.02	5.99	6.19	6.66	5.81	5.97	6.52	7.15	6.81	6.89	6.95	6.42
0.01	6.22	6.90	7.53	7.48	8.32	7.29	8.11	7.78	8.48	9.05	9.23
0.00	9.21	9.00	9.13	9.37	9.38	8.33	9.47	8.98	9.86	10.20	10.67
G3/G2	**0.00**	**0.01**	**0.02**	**0.03**	**0.04**	**0.05**	**0.06**	**0.07**	**0.08**	**0.09**	**0.10**

3. Unbinned, MV ≥ 3, crystalline rocks

0.25	161.8	162.2	159.7	160.0	156.1	154.0	154.0	150.3	146.7	144.9	144.8
0.24	144.4	146.1	144.8	144.6	140.0	137.1	136.2	134.3	131.9	129.9	129.2
0.23	128.9	128.9	129.5	127.5	126.7	124.7	123.0	121.6	119.7	117.2	116.9
0.22	115.1	115.5	114.5	113.5	112.6	110.6	109.9	108.0	107.6	106.2	102.6
0.21	102.1	102.5	102.1	101.1	100.7	98.72	96.29	94.34	92.95	91.71	89.97
0.20	91.93	89.79	89.19	87.55	88.62	86.72	85.06	83.94	82.46	81.09	79.22
0.19	77.95	77.38	77.70	77.26	78.11	77.07	75.58	74.28	73.00	70.62	68.89
0.18	69.27	68.94	68.88	67.71	67.20	65.58	64.26	63.64	63.33	62.06	61.43
0.17	61.25	58.87	59.01	58.54	57.58	56.45	56.54	55.13	53.31	52.60	51.14
0.16	50.34	50.79	50.06	50.05	50.34	49.02	47.95	47.03	46.61	45.77	44.19
0.15	43.40	43.39	42.42	42.10	41.48	41.51	41.14	40.20	40.43	38.04	37.36
0.14	36.07	35.71	36.97	36.91	35.96	34.96	34.60	33.49	33.42	32.76	32.30
0.13	31.22	31.24	30.13	29.75	29.25	29.19	30.28	29.95	26.96	27.63	27.28
0.12	25.01	25.64	26.76	25.84	25.07	24.27	24.06	23.99	23.97	23.74	23.98
0.11	22.83	21.90	21.98	21.44	21.36	20.99	20.80	21.06	21.10	20.54	19.23
0.10	18.41	18.47	18.88	18.64	17.90	17.93	18.53	17.58	17.50	17.92	18.10
0.09	15.39	15.61	16.00	16.18	15.79	15.69	16.26	15.42	16.21	16.17	16.38
0.08	14.73	14.52	14.79	14.42	14.87	14.99	14.89	14.76	14.82	15.15	14.83
0.07	13.60	13.76	13.72	14.09	13.80	14.24	14.58	13.45	14.88	15.57	15.44
0.06	14.18	**13.34**	14.00	14.05	13.87	14.40	14.85	14.59	14.88	16.18	15.79
0.05	14.19	14.61	14.83	15.20	15.53	15.45	16.20	16.23	16.30	17.67	17.47
0.04	16.95	16.48	16.56	17.44	17.53	17.07	18.57	18.69	18.51	15.46	19.68
0.03	18.72	19.47	19.58	19.70	20.10	19.89	20.68	21.17	21.79	23.40	23.35
0.02	23.10	21.92	22.92	23.23	22.98	23.20	24.61	24.41	25.50	26.65	26.99
0.01	26.81	27.77	26.65	26.81	27.57	27.71	28.34	28.49	29.55	31.65	32.32
0.00	30.94	32.83	31.70	31.92	32.79	33.00	33.93	35.12	35.12	36.80	37.43
G3/G2	**0.00**	**0.01**	**0.02**	**0.03**	**0.04**	**0.05**	**0.06**	**0.07**	**0.08**	**0.09**	**0.10**